

Characterization of the Fracture Behavior of Glass Fiber Reinforced Thermoplastics Based on PP, PE-HD, and PB-1

Marcus Schoßig,¹ Wolfgang Grellmann,¹ Thomas Mecklenburg²

¹Center of Engineering Sciences, Martin-Luther University Halle-Wittenberg, Halle/Saale D-06099, Germany

²LyondellBasell Industries, Frankfurt D-65926, Germany

Received 20 May 2009; accepted 11 August 2009

DOI 10.1002/app.31271

Published online 7 October 2009 in Wiley InterScience (www.interscience.wiley.com).

ABSTRACT: This article deals with the influence of the polymeric matrix, such as isotactic polypropylene (iPP), polyethylene (PE-HD), and isotactic polybutene-1 (iPB-1), and the glass fiber content on the material behavior of short glass fiber reinforced thermoplastics. The glass fiber content of all materials ranged between 0 and 50 wt %, which corresponds to a volume content between 0 and approx. 0.264. To describe the mechanical properties of all materials, the stiffness, strength, hardness, and toughness behavior were determined. The crack toughness behavior regarding unstable crack propagation was also assessed by applying fracture mechanics concepts. It was found that the energy-determined *J*-values for the PP material system

reach their maximum at a glass fiber content of 0.135. In contrast, the crack toughness of the PE-HD materials increases continuously with increasing glass fiber content due to the unchanged deformation ability at simultaneously increasing strength. The toughness level of the PB-1 materials is nearly the same independent of the glass fiber content due to the opposite trend of the load and the deformation ability. © 2009 Wiley Periodicals, Inc. *J Appl Polym Sci* 115: 2093–2102, 2010

Key words: fracture mechanics; short glass fiber reinforced polyolefins; instrumented *Charpy* impact test (ICIT); instrumented hardness measurement

INTRODUCTION

For many decades fibers have been applied very successfully to the improvement of the properties of polymeric materials. In this context, the improvement of mechanical properties, i.e. strength and modulus of elasticity as measures of material stiffness and toughness, have been in the focus of opening new fields of application or of replacing nonpolymeric materials.^{1–5} By assessing its strength and stiffness, its hardness and its toughness with instrumented testing methods, it is possible to characterize the material in a comprehensive way.

Usually, the reinforcement of a polymer with fibers results in an increased modulus of elasticity, increased strength, and complex toughness behavior. In the literature, opposing results regarding toughness behavior have been reported. Depending on the glass fiber content, toughness may increase, decrease or be constant for different materials.^{6–8} In either case, fracture toughness and impact resistance are important properties of polymers^{9,10}; hence, it is necessary to quantify their toughness behavior by using suitable and reliable methods of polymer testing and

polymer diagnostics. Particularly, the fracture mechanics assessment of the material's toughness by using the instrumented *Charpy* impact test (ICIT) results in a structure-sensitive evaluation of the material's behavior. With geometry independent fracture mechanics parameters, the characterization of the material's resistance against crack initiation and propagation is possible.^{11–14}

Thermoplastics, such as polypropylene (PP), polyethylene (PE-HD) and polybutene-1 (PB-1) have a versatile application spectrum and they have therefore been adequately scientifically examined.^{15–19} PP materials, which contain short glass fibers are most used in the automotive industry, for household and industrial appliances as well as for applications that require enhanced mechanical properties. For PE-HD and PB-1, the use of glass fibers is relatively uncommon. Nonreinforced PE-HD is mainly used for household goods, piping systems, semi-finished parts, etc. while PB-1 has been used so far only for piping systems and peel foils.²⁰

EXPERIMENTAL

Materials

Neat isotactic PP, PE-HD, and isotactic PB-1, as well as the related short glass fiber reinforced materials (PP/GF, PE-HD/GF, PB-1/GF) were provided by Lyondellbasell Industries (FRANKFURT, Germany).

Correspondence to: M. Schoßig (marcus.schossig@iw.uni-halle.de).

TABLE I
Glass Fiber Content of the Materials in Weight and Volume Content, Respectively

Material	Glass fiber content in weight content Ψ (-)	Glass fiber content in volume content ϕ_V (-)
PP	0	0
	0.1	0.039
	0.2	0.083
	0.3	0.135
	0.4	0.193
PE-HD	0.5	0.264
	0	0
	0.1	0.041
	0.2	0.087
	0.3	0.140
PB-1	0.4	0.201
	0.5	0.273
	0	0
	0.1	0.040
	0.2	0.085
	0.3	0.136
	0.4	0.196
	0.5	0.266

In Table I, the weight and volume content of the glass fibers for the different materials are given and in Table II, some properties of the materials reinforced with 20 wt % fibers are listed. The diameter and the average length of the used glass fibers (E-glass) were approx. 13 μm and 250–425 μm , respectively; this means that the aspect ratio ranged between 20 and 30. For all materials, maleic anhydride grafted coupling agents in a comparable concentration was used to improve the adhesion between the fibers and the polymeric matrix. For the assessment of the bonding conditions between the fibers and the matrix, SEM investigations for the PP, PE-HD, and PB-1 materials with 20 wt % glass fibers were carried out. Figure 1 shows examples of the resulting SEM micrographs. Figure 1(a,b) illustrate good wetting of the glass fibers in the PP/GF system and thus, good bonding of the fibers to the matrix. This leads to a good load transfer between the fibers and the matrix under mechanical stress and thus to a higher load-bearing capacity of such materials. Compared to the PP/GF material, a lower surface coating of the fibers and therefore a diminished

fiber–matrix bonding can be observed for the PE-HD/GF and PB-1/GF materials [Fig. 1(c–f)] due to nonoptimized coupling agents in these systems.

INSTRUMENTATION

Mechanical basic characterization

The basic assessment of the mechanical properties of all materials included quasistatic tensile tests, hardness testing, and *Charpy* impact tests. For selected materials, high-speed tensile tests were performed. The results are published in detail in Ref. 22.

The tensile tests were carried out according to ISO 527-1 by using the universal testing machine *Zwick Z020*. As a result of these tests, the modulus of elasticity E_t and the tensile strength σ_M were determined.²³ For each material, five specimens were tested at room temperature under standard conditions. For all tests, multipurpose test specimens Type 1A with a total length of $l_3 = 170$ mm were used.²⁴ According to ISO 527-1, the test speeds for the measurements of the elasticity and strength were 1 mm/min and 50 mm/min, respectively.

By using the instrumented microhardness tester *Fischerscope H 100c*, the *Martens* hardness (HM) was determined, following ISO 14,577 and eq. (1), where F is the load and h is the indentation depth. For the tests, which were carried out at room temperature, a *Vickers* indenter with a contact area $A_s(h)$ of 26.43 h^2 was used. The load range was between 0.4 and 1000 mN, and HM was determined at the maximum load.

$$HM = \frac{F}{A_s(h)} \quad (1)$$

For the characterization of the toughness properties, the common, conventional *Charpy* impact test was used. Testing was carried out at room temperature by using a *Zwick* pendulum impact tester *HIT5.5P*, following ISO 179-1.²⁵ The three-point bend specimens (80 \times 10 \times 4 mm³) were prepared from multipurpose test specimens, and the loading of the specimens occurred edgewise. Both unnotched and notched specimens were tested. The notches with a notch radius of 0.25 mm and a depth of 2 mm

TABLE II
Density and Thermal Properties of the Materials Reinforced with 20 Wt % Percent Short Glass Fibers [$\Delta H_m^0 = 141$ J/g for PB-1, according to Ref. 21]

Material	Density ρ (g/cm ³)	Melt volume-flow rate MVR _{230/2,16} (cm ³ /10 min)	Heat distortion temperature HDTB (°C)	Melting temperature T_{pm} (°C)	Degree of crystallinity χ (%)
PP/20	1.038	6.3	152.9	165.2	31.9
PE-HD/20	1.094	6.8	122.6	130.5	49.1
PB-1/20	1.060	4.9	115.9	124.8	37.4

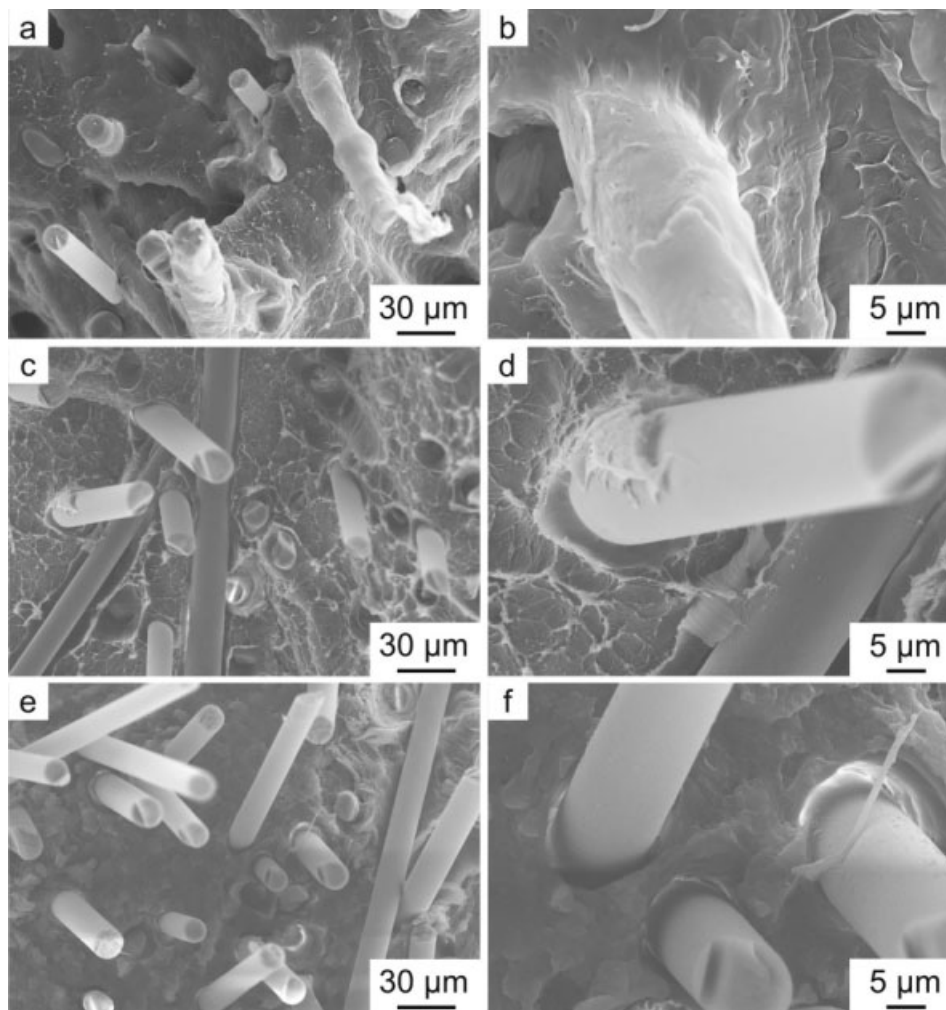


Figure 1 SEM micrographs of PP (a,b—detail), PE-HD (c,d—detail), and PB-1 (e,f—detail) with a weight content of 0.2.

(notch Type A according to ISO 179-1) were produced with the help of the motor driven constant profile knife *Notchois* (CEAST S.P.A, PIANEZZA, ITALY). *Charpy* impact strength a_{cU} and notched *Charpy* impact strength a_{cN} were calculated by

$$a_{cU} = \frac{W_c}{h \times b} \quad (2)$$

and

$$a_{cN} = \frac{W_c}{h \times b_N} \quad (3)$$

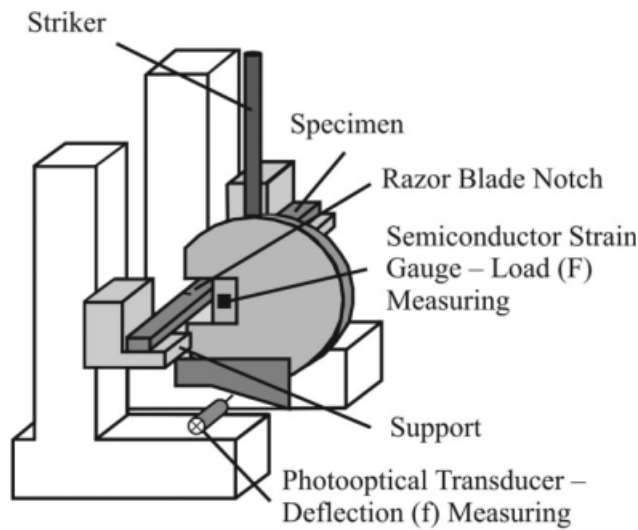
respectively, where b is the specimen width of the unnotched specimen, b_N the remaining width of the notched specimen at the notch, W the absorbed energy, and h the specimen thickness. Furthermore, the ratio of a_{cN} and a_{cU}

$$k_z = \frac{a_{cN}}{a_{cU}} \quad (4)$$

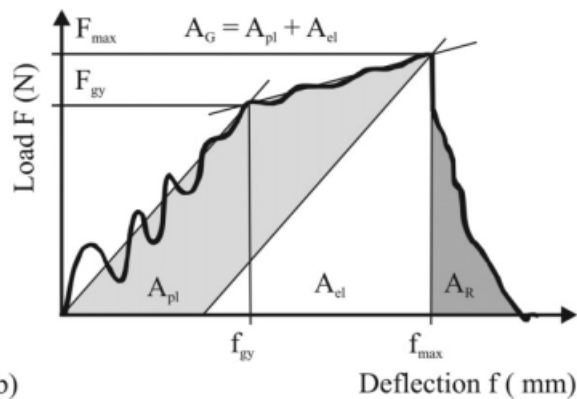
provides information about the notch sensitivity k_z of the materials.

Fracture mechanical investigations

Within the scope of the experimental work, a comprehensive fracture mechanics characterization of the materials based on instrumented *Charpy* impact tests (Fig. 2) was done. As a result of the investigations, the materials' resistance against unstable crack propagation was determined. The experiments and the analysis of the load (F)–deflection (f) diagrams were performed according to an accredited in-house standard.²⁶ According to Ref. 26, single-edge-notched bend specimens with a length $L = 80$ mm, a width $W = 10$ mm, and a thickness $B = 4$ mm were used. The notches were produced by means of a manual notching device with a razorblade having a blade tip radius r of approximately $0.3 \mu\text{m}$. Initial crack length a was 2 mm, which corresponds to a ligament length of 8 mm and an a/W ratio of 0.2, respectively. To ensure comparable conditions for all specimens, they were stored in standard conditions (16 h at 23°C and 50% humidity). The analyses were carried out by using an instrumented *Charpy* impact tester with a maximum work capacity of 4J. Support



a)



b)

Figure 2 Schematic illustration of the fracture mechanics test bench (Instrumented Charpy Impact tester (ICIT-4J)) (a) and a typical load–deflection diagram for an elastic–plastic material behavior (b).

span s was 40 mm and test speed v was 1.5 m/s, which corresponds to a falling angle of 60° .

Beside a schematic representation of the experimental setup, Figure 2(b) shows a typical F – f diagram for elastic–plastic material behavior. Usually, the analysis of the diagrams includes the determination of load F_{gy} and corresponding deflection f_{gy} at the point, where the linear elastic material behavior changes to an elastic–plastic one. Furthermore, maximum load F_{max} and maximum deflection f_{max} are determined. In this way, the impact energy can be divided into different parts, as shown in Figure 2(b). This procedure allows for the calculation of the fracture mechanics parameters, namely fracture toughness K_{Id} , critical crack tip opening displacement δ_{Id} and critical J -values J_{Id}^{ST} according to the following equations:

$$K_{Id} = \frac{F_{max} \times s}{B \times W^{3/2}} \times f\left(\frac{a}{W}\right) \quad (5)$$

$$\delta_{Id} = \frac{1}{n} \times (W - a) \times \frac{4 \times f_{max}}{s} \quad (6)$$

$$J_{Id}^{ST} = \eta_{el} \times \frac{A_{el}}{B(W - a)} + \eta_{pl} \times \frac{A_{pl}}{B(W - a)} \times \frac{W - a_{eff}}{W - a} \quad (7)$$

where, n is the rotational factor, which is four at the moment of fracture,²⁷ $f(a/W)$, η_{el} and η_{pl} are geometry functions, a_{eff} is the effective crack length, and A_{el} and A_{pl} the elastic and plastic part of the total deformation energy, respectively. Detailed information on geometry functions $f(a/W)$, η_{el} and η_{pl} can be found in.^{11–14,26–28}

For the verification of the geometry independence of the fracture mechanics parameters, the following inequations (8–10) were used. If the inequations are fulfilled, geometry independence can be assumed. Further details regarding this subject are given in.^{29,30}

$$B; a; (W - a) \geq \beta \left(\frac{K_{Id}}{\sigma_d} \right)^2 \quad (8)$$

$$B; a; (W - a) \geq \xi \delta_{Id} \quad (9)$$

$$B; a; (W - a) \geq \varepsilon \frac{J_{Id}}{\sigma_d} \quad (10)$$

where, σ_d is the yield strength at a test speed of 1.5 m/s, and β , ξ , and ε are geometrical factors. The fracture mechanics values are geometry independent if the above inequations are fulfilled.

RESULTS AND DISCUSSION

Mechanical characterization

The results of the tensile tests in form of the modulus of elasticity E_t and tensile strength σ_M are represented in Figure 3. With increasing glass fiber content, the modulus of elasticity increases linearly for all polyolefin materials. The stiffness level of the PP materials is the highest compared to that of the PE-HD and PB-1 systems. Already the comparison of the neat polymers shows that there are differences between the three materials. PP has the highest value of E_t , followed by PE-HD. These differences in the parameter level of E_t between the materials remain when glass fibers are added. In contrast to the modulus of elasticity of neat PE-HD and PB-1, tensile strength σ_M is on the same level in both materials. However, the addition of glass fibers to PB-1 leads to a stronger increase in σ_M , which is more pronounced compared to PE-HD. Furthermore, tensile strength σ_M vs. glass fiber content increases nonlinearly for all materials examined. Again, the

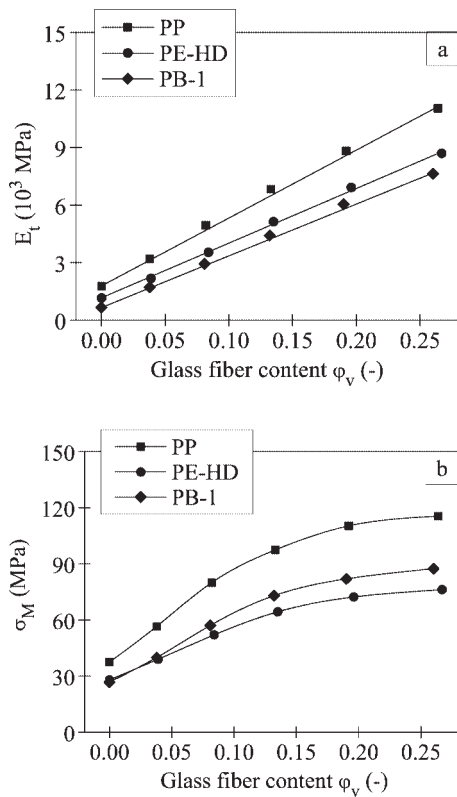


Figure 3 Modulus of elasticity E_t (a) and tensile strength σ_M (b) in dependence on the glass fiber ϕ_v (-).

highest strength values were determined for the PP system.

The results of the instrumented microhardness measurements are shown in Figure 4. For all composites, HM was found to be continuously rising with increasing glass fiber content. The highest hardness values were determined for the PP materials, compared to the PE-HD and PB-1 systems. For the latter, the hardness level remains nearly the same, independent of the glass fiber content.

Furthermore, as reported earlier, *Charpy* impact strength a_{cU} and notched *Charpy* impact strength a_{cN}

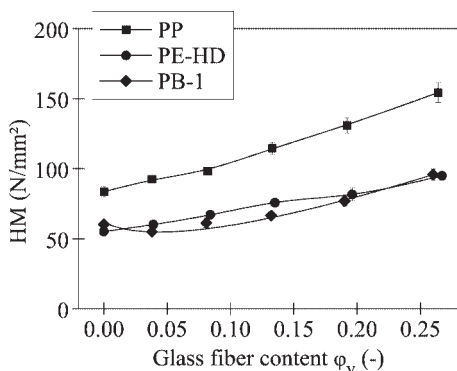


Figure 4 Martens hardness (HM) for all composites in dependence on the glass fiber content.

were determined. The results are shown in Figure 5, where a_{cU} and a_{cN} are plotted as a function of the glass fiber content. The unnotched specimens of the nonreinforced polymers could not be broken with the selected experimental set up (maximum working capacity of 4J); therefore, no valid impact strength values could be determined according to ISO 179-1. This is marked with “nb” in Figure 5(a). For all reinforced materials, a failure behavior was observed, which is characterized by a complete fracture (Type C in ISO 179-1). The highest toughness level could be found for the PP materials. Furthermore, for the PP and the PB-1 material systems, an increase in *Charpy* impact strength a_{cU} due to the increasing addition of glass fibers was observed. However, more or less pronounced maximum values were found at a glass fiber content of 0.135 for PP and of 0.19 for PB-1, respectively. In contrast to these results, the a_{cU} values of the PE-HD glass fiber composites are almost constant with increasing glass fiber content. The results of the notched *Charpy* impact test are somewhat different [Fig. 5(b)]. While for the PP and PE-HD systems, a strong increase in a_{cN} was found up to a volume content of 0.135 and 0.140, respectively, the PB-1 system shows a strong decreasing toughness upto a glass fiber content of

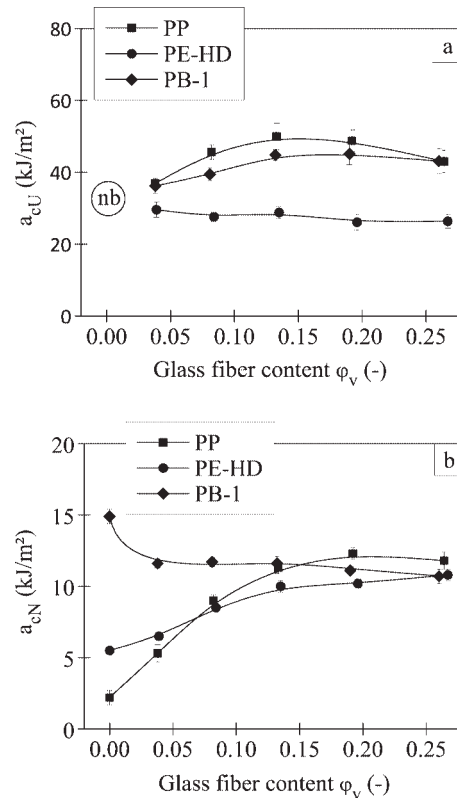


Figure 5 *Charpy* impact toughness a_{cU} (a) and notched *Charpy* impact toughness a_{cN} (b) of the PP, PE-HD, and PB-1 composites as a result of the conventional *Charpy* impact test (nb-not broken).

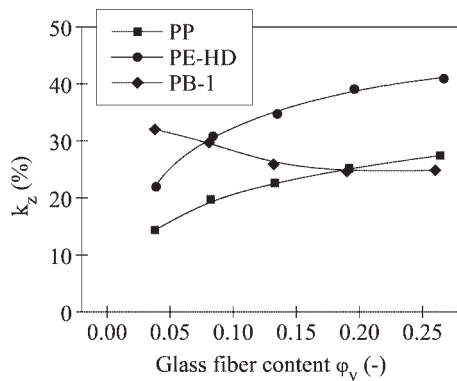


Figure 6 Notch sensitivity k_z as a function of glass fiber content.

0.040. From 0.085 upto 0.266 a further, but smaller decrease of the toughness occurred.

The different behavior of a_{cU} and a_{cN} is an indication for a difference in the notch sensitivity of the materials. For this reason, notch sensitivity k_z as an important criterion for product design was calculated when both values a_{cU} and a_{cN} were available. The results are represented in Figure 6. As it can be seen, the notch sensitivity of the PP and PE-HD systems increases qualitatively in the same way as a_{cN} . Again, the PB-1 system is different, because it is characterized by a decrease in notch sensitivity with

increasing glass fiber content. The highest notch sensitivity was found for the PE-HD system.

Fracture mechanics characterization

As mentioned above, the analysis of the F - f diagrams from instrumented *Charpy* impact tests allows for the determination of various fracture mechanics parameters. The following is a summary and discussion of the results of such tests with the different materials. At first, Figure 7(a–d) show fracture toughness K_{Id} , critical crack tip opening displacement δ_{Id} , and the δ_{Id} values in dependence on the glass fiber content for all materials, as well as selected load-deflection diagrams.

In comparison to PE-HD and PB-1, the PP materials exhibit the highest K_{Id} values [Fig. 7(a)]. This can be explained by the considerably higher load-bearing capacity of PP due to the good glass fiber bonding (SEM micrographs in Fig. 1). For PE-HD and PB-1, an almost identical increase in the K_{Id} values as a function of the glass fiber content was detected, with insignificantly higher values for the PB-1 materials.

The results for critical crack tip opening displacement δ_{Id} as a deformation-determined fracture mechanics parameter are represented in Figure 7(b). An increase in critical crack tip opening

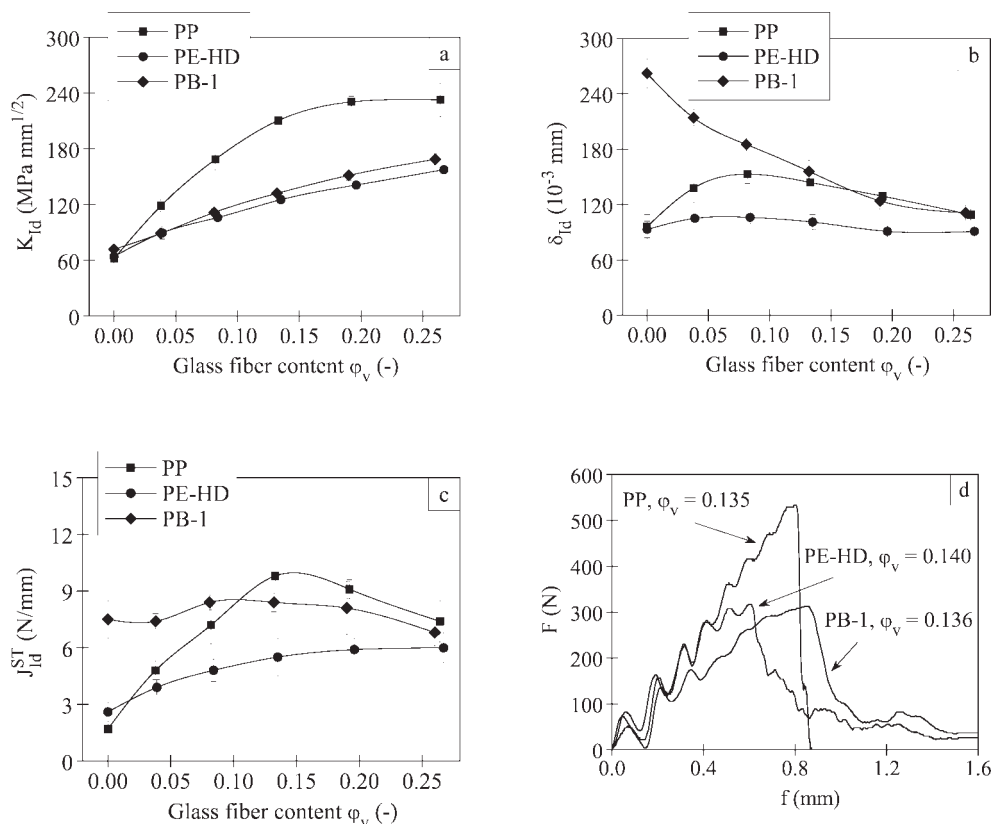


Figure 7 Fracture toughness K_{Id} (a) critical crack tip opening displacement δ_{Id} (b) and J -values J_{Id}^{ST} (c) for all materials as well as selected load-deflection (F - f) diagrams (d).

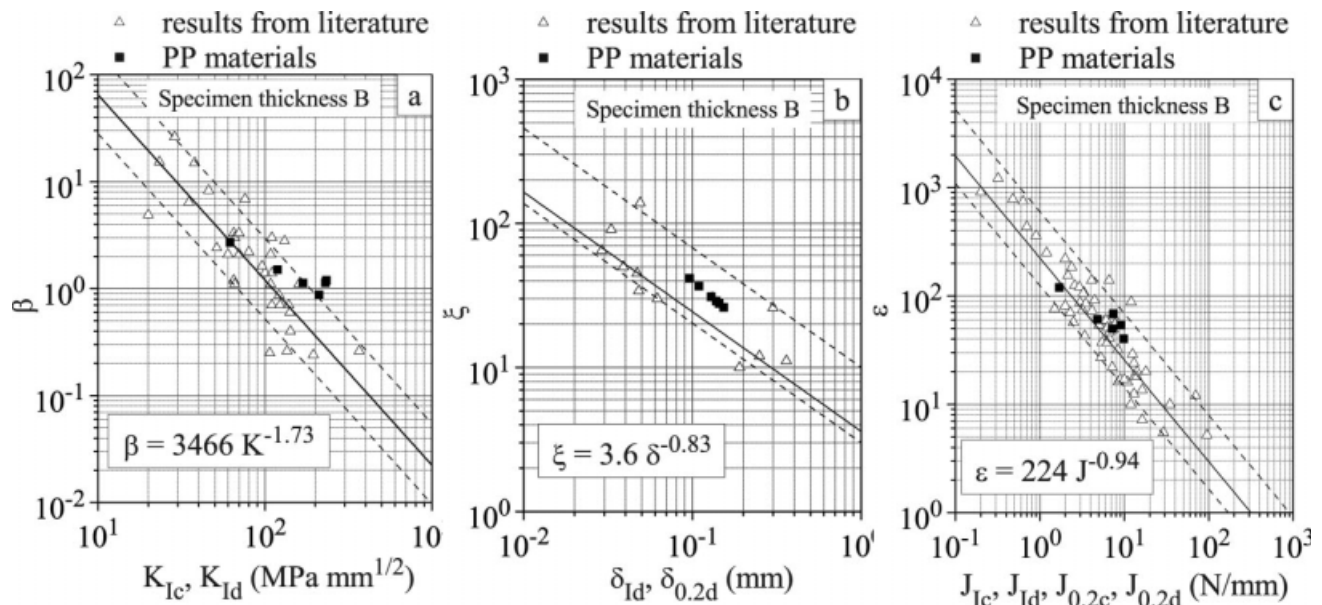


Figure 8 Geometrical factors β , ξ , and ϵ for all PP materials examined; literature results were taken from Ref. 29.

displacement δ_{Id} upto glass fiber content of 0.083 is characteristic for the PP materials. Further reinforcement leads to the reduction in the material's deformation ability and therefore to a decrease in the δ_{Id} values. For the PE-HD materials, the critical crack tip opening displacement changes only insignificantly with increasing glass fiber content. Furthermore, a continuous decrease in δ_{Id} is noticeable in the PB-1 system, which can be explained by a reduction in deformation ability occurring at higher glass fiber content.

In contrast to load-determined parameter K_{Id} and deformation-determined parameter δ_{Id} , the application of the J integral concept of the elastic-plastic fracture mechanics provides the opportunity to analyze the fracture process from the energetic point of view. The J -values represented here were calculated according to the evaluation method of *Sumpter and Turner*; results are shown in Figure 7(c). At first, the comparison of the J_{Id}^{ST} values of the neat polymers shows clear differences between the matrix materials. The crack toughness of PB-1 is considerably higher than that of PP and PE-HD. The addition of the glass fibers resulted in changes in the crack toughness behavior of each material system.

A clear increase in crack toughness as resistance against unstable crack propagation expressed as J_{Id}^{ST} is noticeable in the PP materials with the addition of glass fiber upto a content of 0.135. This is attributed to both the higher load capacity and the increase in deformation ability. After reaching a maximum at 0.135, a decrease in J_{Id}^{ST} can be observed with increasing glass fiber content. The reason for this is the reduction in deformation ability. This means that there is an optimal toughness level for this material

system at the glass fiber content of 0.135. Generally, it can be concluded that the deformation behavior of the PP material system is load-determined up to a glass fiber content of 0.135, and deformation-determined at higher contents 0.193 and 0.264. The J_{Id}^{ST} values of the PE-HD system show an increase in crack toughness with increasing glass fiber content, as well. From the dependence of K_{Id} and δ_{Id} , it can be derived that the reinforced PE-HD system shows load-determined deformation behavior. When the glass fiber content in the PB-1 materials is increased, the deformation behavior is characterized by an increasing maximum load and a decreasing maximum deflection. For this reason, crack toughness J_{Id}^{ST} is relatively little affected by the addition of glass fibers due to the superposition of load and deformation influence. Only a rather insignificant maximum of J_{Id}^{ST} at a glass fiber content of 0.085–0.136 was found.

The differences in the deformation behavior of the three different material systems is illustrated by Figure 7(d) showing selected load-deflection diagrams of the materials reinforced with approx. 0.14 short glass fibers. It can be seen that the PP material is characterized by a linear elastic behavior with unstable crack propagation. The latter is indicated by the distinct drop of the load after reaching the maximum load. In contrast, from the existence of yield point F_{gy} , an elastic-plastic behavior is noticeable in the PE-HD and PB-1 materials. The fracture process for these materials is also characterized by an additional crack propagation energy A_R [schematic illustration in Fig. 2(b)]. From the differences between the conventional toughness and the fracture mechanics values, it can be concluded that applying the

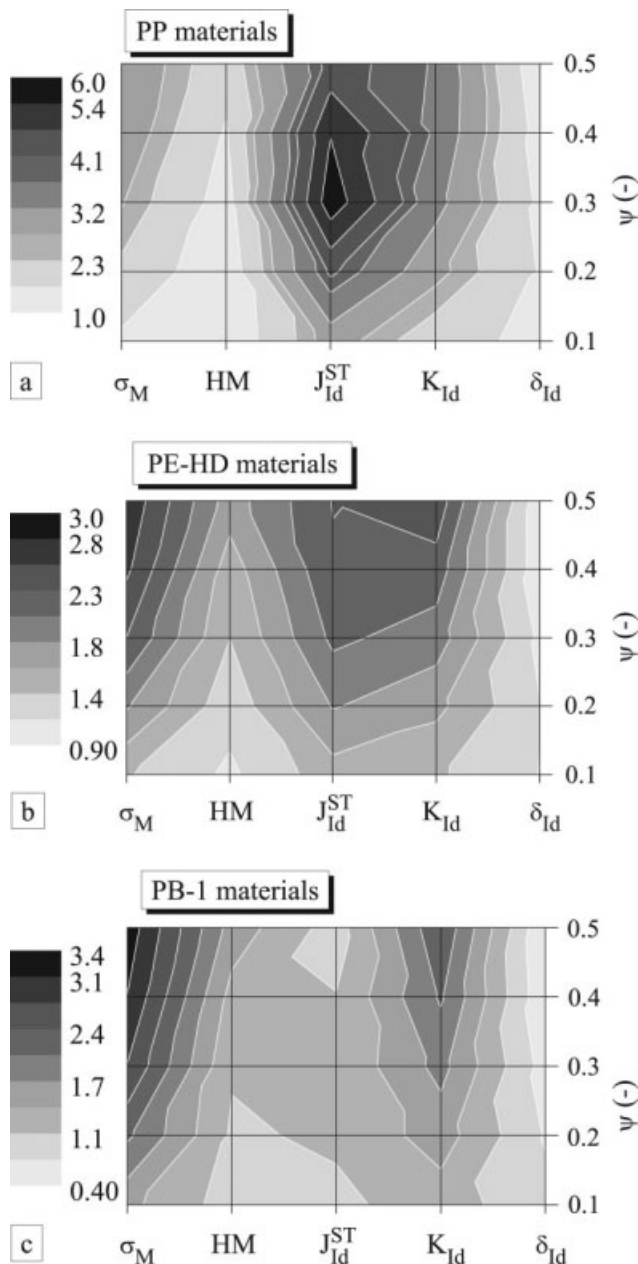


Figure 9 Comparison of the normalized mechanical parameters.

notched *Charpy* impact test only would lead to an overestimation of the toughness in the case of the PE-HD and PB-1 materials. The reason for this is the integral character of notched *Charpy* impact strength a_{cN} . As a consequence, the application of instrumented methods of polymer diagnostics should be an essential part of research and development.

In general, fracture mechanics material parameters are independent of geometry if a plane strain state is ensured. As described within the experimental part of this article, the specimen geometry has to fulfill some requirements.^{28–30} For checking the geometry independence, the geometrical factors β , ξ , and ε

were determined after rearranging eq. (8–10). This analysis was done for B , a , and $(W-a)$, and all materials separately. Figure 8 shows the results for specimen thickness B , using the PP materials as an example. Similar results were obtained for a and $(W-a)$, as well as for the PE-HD and PB-1 materials. In general, all crack toughness values, below illustrated as straight lines, are dependent on specimen geometry. As shown in,³⁰ a scatter band can be fixed according to the experimental results for which geometry independence is guaranteed. Thus, all fracture mechanics parameters being inside the scatter band or above the straight line drawn in Figure 8 are geometry independent. Consequently, geometry independence can be assumed for all fracture mechanics parameters determined. This is a very important aspect when using these parameters for construction or simulation, for example.

Identification of the optimal glass fiber content

To summarize, for each material system investigated, the reinforcement with short glass fibers is affected in a different way. For the assessment of the optimal glass fiber content, the mechanical parameters were normalized and compared to the neat materials. Figure 9 shows the results for the tensile

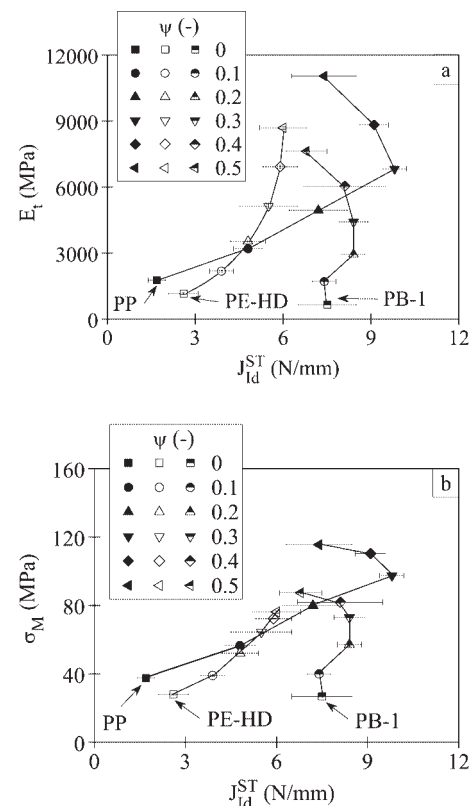


Figure 10 Stiffness–toughness and strength–toughness balance in the form of modulus of elasticity E_t (a) and tensile strength σ_M (b) versus J_{Id}^{ST} for all material systems.

strength, the *HM*, as well as the fracture mechanics parameters of all materials in form of a contour plot. For the PP system, an increase in mechanical and fracture mechanics properties can be achieved by the addition of glass fibers, especially in the J_{Id}^{ST} values. In comparison to the neat material, J_{Id}^{ST} increases by a factor of six for a glass fiber content of 0.135, which corresponds to a weight content of 0.3. As a consequence, considering all mechanical and fracture mechanics parameters, an optimal property level of the PP materials is achieved at a glass fiber content of 0.135. A different material behavior was obtained for the PE-HD and PB-1 systems. Compared to the neat materials, the highest increase in mechanical and fracture mechanics parameters were found for the tensile strength and for the load-determined fracture toughness. Thus, the highest fiber content leads to a reinforcement factor of 3.0 for the PE-HD system and of 3.4 for the PB-1 system.

In addition, the assessment of the stiffness–toughness balance and strength–toughness balance, respectively, is important. Figure 10 shows the interrelationships between modulus of elasticity E_t and tensile strength σ_M vs. the J_{Id}^{ST} values. For the PP materials, an optimal balance between stiffness, strength, and crack toughness is found at a glass fiber content of 0.135. In contrast, for the PE-HD system an increase in stiffness, strength, as well as toughness with higher fiber contents is characteristic. This observation is consistent with the results of the comparison of the mechanical parameters described earlier. Also for the PB-1 system, an optimal balance at glass fiber contents of 0.085 and 0.135, which corresponds to a weight content of 0.2 and 0.3, is noticeable, similar to that of the PP materials. This is in contrast to the information obtained through the comparison of the mechanical parameters, and emphasizes the importance of a multiparametric description of the material's behavior.

CONCLUSIONS

This article comprises results of mechanical and fracture mechanics investigations of short glass fiber reinforced PP, PE-HD, and PB-1 materials. For the assessment of the mechanical properties, modulus of elasticity, strength, microhardness, and toughness parameters were determined. In principle, the level of the mechanical parameters is enhanced with increasing glass fiber content. The highest level of mechanical parameters was observed for the PP material system.

When assessing crack toughness by means of different fracture mechanics concepts, a more complex behavior was found. For the various material systems, optimum glass fiber content was found. This is due to the rising load-bearing capacity of the materials when

the amount of glass fibers is increased. At the same time, the deformation ability of the material is reduced. However, the value of the optimum glass fiber content depends on the matrix material. While for the PP/glass fiber composites the optimal toughness level was achieved at a glass fiber content of 0.135, for the PB-1 systems, J_{Id}^{ST} values, which consider the load and deformation in form of superposition, show only an insignificant increase in toughness at a glass fiber content of 0.085 and 0.136, respectively. For the PE-HD materials, a continuous increase of the toughness in dependence on the glass fiber content was found. Therefore, also differences in the balance of strength, stiffness, and toughness occurred.

References

1. Friedrich, K., Ed. *Application of Fracture Mechanics to Composite Materials*; Elsevier Science Publishers B.V.: Amsterdam, 1989.
2. Roulin-Moloney, A. C., Ed. *Fractography and Failure Mechanisms of Polymers and Composites*; Elsevier Science: London, New York, 1989.
3. Jones, R. F. *Guide to Short Fiber Reinforced Plastics*; Carl Hanser Verlag: Munich, 1998.
4. Karger-Kocsis, J. In *Polymer Blends*; Paul, D. R., Bucknall, C. B., Eds.; Wiley: New York, Chichester, Weinheim, Brisbane, Singapore, Toronto, 2000; Vol. 2, Chapter 31, p 395.
5. Grellmann, W.; Seidler, S. *J Polym Eng* 1992, 11, 71.
6. Karger-Kocsis, J. In *Application of Fracture Mechanics to Composite Materials*; Friedrich, K., Ed.; Elsevier Science Publishers B.V.: Amsterdam, 1989; Chapter 6, p 189.
7. Seidler, S.; Grellmann, W. *Zähigkeit von Teilchengefüllten und Kurzfaserverstärkten Polymerwerkstoffen*; Fortschritt-Berichte VDI—Reihe 18: Mechanik/Bruchmechanik Nr. 92: Düsseldorf, 1991.
8. Gomina, M.; Pinot, L.; Moreau, R.; Nakache, E. In *Fracture of Polymers, Composites and Adhesives II*; Blackmann, B. R. K., Pavan, A., Williams, J. G., Eds.; Elsevier: Amsterdam, 2003; ESIS Publ. 32, p 399.
9. Bucknall, C. B. *Toughened Plastics*; Applied Science Publishers: London, 1977.
10. Paul, D. R.; Bucknall, C. B. *Polymer Blends*; Wiley-Interscience: New York, 2000; Vol. 2.
11. Anderson, T. L. *Fracture Mechanics—Fundamentals and Applications*; Taylor & Francis Group: Boca Raton, London, New York, Singapore, 2005.
12. Grellmann, W.; Seidler, S., Eds. *Deformation and Fracture Behaviour of Polymers*; Springer-Verlag: Berlin, Heidelberg, 2001.
13. Grellmann, W.; Seidler, S., Eds. *Polymer Testing*; Carl Hanser Verlag: Munich, 2007.
14. Seidler, S.; Grellmann, W. *Polym Test* 1995, 14, 453.
15. Karger-Kocsis, J. *Polypropylene an A-Z Reference*; Kluwer Academic Publishers: Dordrecht, 1999.
16. Peacock, A. J. *Handbook of Polyethylene: Structures, Properties, and Applications*; Marcel Dekker: New York, 2000.
17. Kalay, G.; Kalay, C. R. *J Appl Polym Sci* 2003, 88, 814.
18. Kopp, S.; Wittmann, J. C.; Lotz, B. *J Mater Sci* 1994, 29, 6159.
19. Shieh, Y.-T.; Lee, M.-S.; Chen, S.-A. *Polymer* 2001, 42, 4439.
20. Nase, M.; Androsch, R.; Langer, B.; Baumann, H.-J.; Grellmann, W. *J Appl Polym Sci* 2008, 107, 3111.
21. Alfonso, G. C.; Azzurri, F.; Castellano, M. *J Therm Anal Calorim* 2001, 66, 197.

22. Schoßig, M.; Bierögel, C.; Grellmann, W.; Mecklenburg, T. *Polym Test* 2008, 27, 893.
23. ISO 527-1, *Plastics—Determination of tensile properties—I. General principles*, ISO 527-1, 1993.
24. ISO 527-2, *Plastics—Determination of tensile properties—II. Test conditions for moulding and extrusion plastics*, ISO 527-2, 1993.
25. ISO 179-1, *Plastics—Determination of Charpy properties—III. Non-instrumented impact test*, ISO 179-1, 2000.
26. Grellmann, W.; Seidler, S.; Hesse, W. *Testing of plastics—instrumented Charpy impact test (ICIT)—Procedure for determining the crack resistance behaviour using the instrumented impact test*. MPK-ICIT: 2007-01 Part I and Part II, Available at http://www2.iw.uni-halle.de/ww/mpk/p_e.pdf.
27. Jungbluth, M. *Untersuchungen zum Verformungs- und Bruchverhalten von PVC-Werkstoffen*, Dissertation, Technischen Hochschule "Carl Schorlemmer" Leuna-Merseburg, 1987.
28. Grellmann, W.; Seidler, S.; Hesse, W. In *Deformation and Fracture Behaviour of Polymers*; Grellmann, W., Seidler, S., Eds.; Springer: Berlin, Heidelberg, 2001; p 71.
29. Grellmann, W.; Lach, R.; Seidler, S. *Int J Fract* 2002, 118, L9.
30. Grellmann, W.; Seidler, S.; Lach, R. *Materialwiss Werkst* 2001, 32, 552.